

Dynamical aspects of equilibrium and off-equilibrium simulations of a three-dimensional Heisenberg spin glass

H. Kawamura

Kyoto Institute of Technology, Sakyo-ku, Kyoto 606-8585, Japan

and

K. Hukushima

ISSP, University of Tokyo, Minato-ku, Tokyo 106-8666, Japan

Spin-glass and chiral-glass orderings of a three-dimensional isotropic Heisenberg spin glass are studied both by equilibrium and off-equilibrium Monte Carlo simulations with emphasis on their dynamical aspects. The model is found to exhibit a finite-temperature chiral-glass transition without the conventional spin-glass order. Although chirality is an Ising-like quantity from symmetry, universality class of the chiral-glass transition appears to be different from that of the standard Ising spin glass. In the off-equilibrium simulation, while the spin autocorrelation exhibits only an interrupted aging, the chirality autocorrelation persists to exhibit a pronounced aging effect reminiscent of the one observed in the mean-field model.

1. Introduction

Ordering of complex systems has attracted interest of researchers working in the field of numerical simulations. Well-known examples of such complex systems may be a variety of glassy systems including window glasses, orientational glasses of molecular crystals, vortex glasses in superconductors and spin-glass magnets. Often, in the dynamics of such complex systems, characteristic slow relaxation is known to occur. It has been a great challenge for researchers in the field to clarify the nature and the origin of these slow dynamics, as well as to get fully equilibrium properties by overcoming the slow relaxation. In particular, *spin glasses* are the most extensively studied typical model system, for which numerous analytical, numerical and experimental works have been made.¹

Studies on spin glasses now have more than twenty years of history. Main focus of earlier studies was put on obtaining the equilibrium properties of spin glasses. While extensive experimental studies have clarified that the spin-glass magnets exhibit an equilibrium phase transition at a finite temperature,¹ the true nature of the experimentally observed spin-glass transition and that of the low-temperature spin-glass phase still remain open problems. It has been known that the magnetic interactions in many of real spin-glass materials are Heisenberg-like, in the sense

that the magnetic anisotropy is much weaker than the exchange energy. In apparent contrast to experiments, numerical simulations have indicated that isotropic Heisenberg spin glass exhibits only a zero-temperature transition.^{2,3,4,5,6,7,8} Apparently, there is a puzzle here: How can one reconcile the absence of the spin-glass order in an isotropic Heisenberg spin glass with the experimental observation?

In order to solve this apparent puzzle, a chirality mechanism of experimentally observed spin-glass transitions was recently proposed by one of the authors,^{6,8} on the assumption that an isotropic 3D Heisenberg spin glass exhibited a finite-temperature *chiral-glass* transition without the conventional spin-glass order, in which only spin-reflection symmetry was broken with preserving spin-rotation symmetry. “Chirality” is an Ising-like multispin variable representing the sense or the handedness of the noncoplanar spin structures. It was argued that, in real spin-glass magnets, the spin and the chirality were “mixed” due to the weak magnetic anisotropy and the chiral-glass transition was then “revealed” via anomaly in experimentally accessible quantities. Meanwhile, theoretical question whether there really occurs such finite-temperature chiral-glass transition in an isotropic 3D Heisenberg spin glass, a crucial assumption of the chirality mechanism, remains somewhat inconclusive.^{8,9}

More recently, there arose a growing interest both theoretically and experimentally in the *off-equilibrium* dynamical properties of spin glasses. In particular, aging phenomena observed in many spin glasses¹⁰ have attracted attention of researchers.^{11,12} Unlike systems in thermal equilibrium, relaxation of physical quantities depends not only on the observation time t but also on the waiting time t_w , *i.e.*, how long one waits at a given state before the measurements. Recent studies have revealed that the off-equilibrium dynamics in the spin-glass state generally has two characteristic time regimes.^{11,12,13} One is a short-time regime, $t_0 \ll t \ll t_w$ (t_0 is a microscopic time scale), called “quasi-equilibrium regime”, and the other is a long-time regime, $t \gg t_w$, called “aging regime” or “out-of-equilibrium regime”. In the quasi-equilibrium regime, the relaxation is stationary and the fluctuation-dissipation theorem (FDT) holds. On the other hand, in the aging regime, the relaxation becomes non-stationary, FDT broken. Although theoretical studies of off-equilibrium dynamics on Ising-like models^{17,13,18,19} succeeded in reproducing some of the features of experimental results, it is clearly desirable to study the dynamical properties of a *Heisenberg* spin-glass model to make a direct link between theory and experiments.

In the present article, we report on our recent results of equilibrium as well as off-equilibrium Monte Carlo (MC) simulations on an isotropic 3D Heisenberg spin glass, with emphasis on their dynamical aspects. Ordering properties of both the spin and the chirality are studied, aimed at testing the validity of the proposed chirality scenario of spin-glass transitions. We note that MC simulation is particularly suited to this purpose, since, at the moment, chirality itself is not directly measurable experimentally. By contrast, it is straightforward to measure the chirality by numerical simulations.

2. Model

The model we simulate is the classical Heisenberg model on a simple cubic lattice with the nearest-neighbor random Gaussian couplings, J_{ij} , defined by the Hamiltonian

$$\mathcal{H} = - \sum_{\langle ij \rangle} J_{ij} \mathbf{S}_i \cdot \mathbf{S}_j, \quad (2.1)$$

where $\mathbf{S}_i = (S_i^x, S_i^y, S_i^z)$ is a three-component unit vector, and the sum runs over all nearest-neighbor pairs with $N = L \times L \times L$ spins. J_{ij} is the isotropic exchange coupling with zero mean and variance J .

Frustration in vector spin systems often causes *noncollinear* or *noncoplanar* spin structures. Such noncollinear or noncoplanar orderings give rise to a nontrivial chirality according as the spin structure is either right- or left-handed.¹⁴ We define the local chirality at the i -th site and in the μ -th direction, $\chi_{i\mu}$, for three Heisenberg spins by,

$$\chi_{i\mu} = \mathbf{S}_{i+\hat{\mathbf{e}}_\mu} \cdot (\mathbf{S}_i \times \mathbf{S}_{i-\hat{\mathbf{e}}_\mu}), \quad (2.2)$$

where $\hat{\mathbf{e}}_\mu$ ($\mu = x, y, z$) denotes a unit lattice vector along the μ -axis. The chirality is a pseudoscalar in the sense that it is invariant under global spin rotation but changes sign under global spin reflection. Chiral order is related to a possible breaking of the spin-reflection symmetry with preserving the spin-rotation symmetry.

3. Equilibrium simulations

First, we report on our *equilibrium* MC simulations of a fully isotropic 3D Heisenberg spin glass defined by Eq. (2.1).⁹ Monte Carlo simulation is performed based on an exchange method developed by Hukushima and Nemoto,¹⁵ where whole configurations at two neighboring temperatures of the same sample are occasionally exchanged keeping the system at equilibrium. The method has turned out to be efficient in thermalizing the system showing slow relaxation over free energy barriers.¹⁵ By this method, we succeed in equilibrating the system down to the temperature considerably lower than those attained in the previous simulations. We run in parallel two independent replicas with the same bond realization and compute an overlap between the chiral variables in the two replicas,

$$q_\chi = \frac{1}{3N} \sum_{i,\mu} \chi_{i\mu}^{(1)} \chi_{i\mu}^{(2)}. \quad (3.1)$$

The lattice sizes studied are $L = 6, 8, 10, 12, 16$ with periodic boundary conditions. In the case of $L = 16$, for example, we prepare 60 temperature points distributed in the range $[0.10J, 0.25J]$ for a given sample, and perform 1.2×10^6 exchanges per temperature of the whole lattices combined with the same number of standard single-spin-flip heat-bath sweeps. For $L = 16$, we equilibrate the system down to the temperature $T/J = 0.10$, which is lower than the minimum temperature attained previously. Sample average is taken over 1500 ($L = 6$), 1200 ($L = 8$),

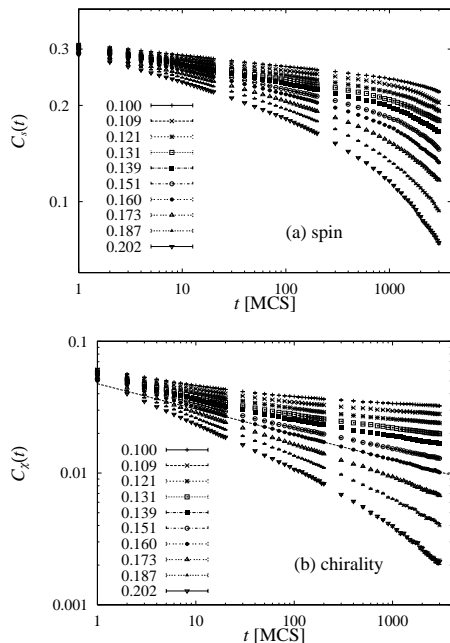


Fig. 1. Log-log plots of the time dependence of the equilibrium spin (a) and chirality (b) autocorrelation functions at several temperatures. The lattice size is $L = 16$ averaged over 64 samples.

640 ($L = 10$), 296 ($L = 12$) and 136 ($L = 16$) independent bond realizations. Equilibration is checked by monitoring the stability of the results against at least three-times longer runs for a subset of samples.

Information about the equilibrium dynamics can be obtained via the spin and chirality autocorrelation functions defined by

$$C_s(t) = \frac{1}{N} \sum_i [\langle \mathbf{S}_i(t_0) \cdot \mathbf{S}_i(t + t_0) \rangle], \quad (3.2)$$

$$C_\chi(t) = \frac{1}{3N} \sum_{i,\mu} [\langle \chi_{i\mu}(t_0) \chi_{i\mu}(t + t_0) \rangle], \quad (3.3)$$

where $\langle \dots \rangle$ and $[\dots]$ represent the thermal average and the average over bond disorder, respectively, while t_0 denotes some initial time at which the system is already fully equilibrated. Although we have used the exchange MC method for thermalizing the system, the time evolution during the measurements of autocorrelations has been made via the standard single-spin-flip heat-bath updating. MC time dependence of the calculated $C_s(t)$ and $C_\chi(t)$ are shown in Figs. 1 on log-log plots for several temperatures. As can be seen from Fig. 1(a), $C_s(t)$ shows a downward curvature at all temperature studied, suggesting an exponential-like decay characteristic of the disordered phase, consistently with the absence of the standard

spin-glass order. In sharp contrast to this, $C_\chi(t)$ shows either a downward curvature characteristic of the disordered phase, or an upward curvature characteristic of the long-range ordered phase, depending on whether the temperature is higher or lower than $T/J \simeq 0.16$, while just at $T/J \simeq 0.16$ the linear behavior corresponding to the power-law decay is observed: See Fig. 1(b). Hence, our dynamical data indicates that the chiral-glass order without the standard spin-glass order takes place at $T_{CG}/J = 0.160 \pm 0.005$, below which a finite chiral Edwards-Anderson (EA) order parameter $q_{CG}^{EA} > 0$ develops. From the slope of the data at $T = T_{CG}$, the exponent λ characterizing the power-law decay of $C_\chi(t) \approx t^{-\lambda}$ is estimated to be $\lambda = 0.193 \pm 0.005$. We note that the occurrence of a chiral-glass transition was also supported by the behaviors of the static Binder ratios (not shown here).⁹

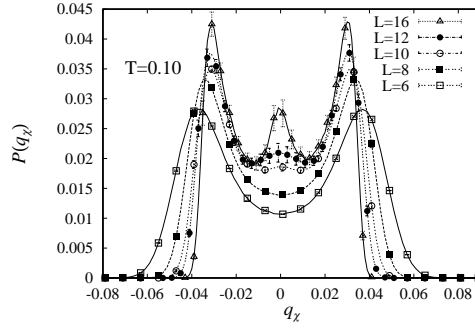


Fig. 2. Chiral-overlap distribution function below T_{CG} . The temperature is $T/J = 0.1$.

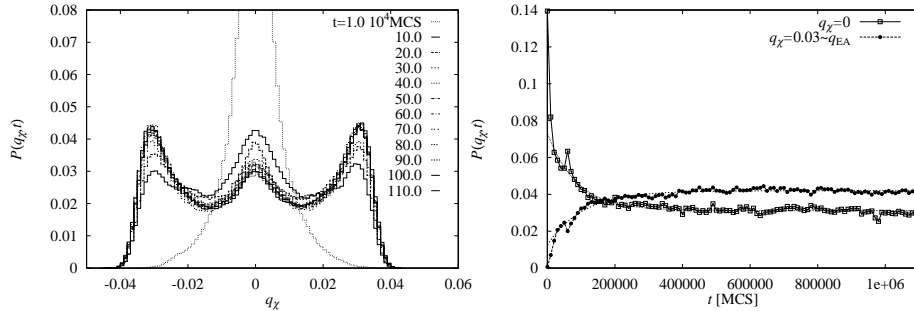


Fig. 3. MC-time evolution of the chiral-overlap distribution function at $T/J = 0.1$ with $L = 16$ (left). MC-time dependence of the height of $P(q_\chi)$ at $q_\chi = 0$ and at $q_\chi \sim q_{EA}$ (right).

Establishing the existence of a finite-temperature chiral-glass transition, we proceed to the study of the properties of the chiral-glass ordered state itself. In Fig. 2, we display the distribution function of the chiral-overlap defined by

$$P(q'_\chi) = [\langle \delta(q_\chi - q'_\chi) \rangle], \quad (3.4)$$

calculated by the exchange MC method at a temperature $T/J = 0.1$, well below the chiral-glass transition temperature. As is evident from Fig. 2, the shape of the calculated $P(q_\chi)$ is somewhat different from the one observed in the standard Ising-like models such as the 3D EA model or the mean-field SK model. As usual, $P(q_\chi)$ has standard “side-peaks” corresponding to the EA order parameter $\pm q_{\text{CG}}^{\text{EA}}$, which grow and sharpen with increasing L . In addition to the side peaks, an unexpected “central peak” at $q_\chi = 0$ shows up for larger L , which also grows and sharpens with increasing L . This latter aspect, *i.e.*, the existence of a central peak growing and sharpening with the system size, is a peculiar feature of the chiral-glass ordered phase never observed in the EA or the SK models. Since we do not find any sign of a first-order transition such as a discontinuity in the energy, the specific-heat nor the order parameter $q_{\text{CG}}^{\text{EA}}$, this feature is likely to be related to a nontrivial structure in the phase space associated with the chirality. We note that this peculiar feature is reminiscent of the behavior characteristic of some mean-field models showing the so-called *one-step replica-symmetry breaking* (RSB).¹ In Figs. 3, we show the (exchange) MC time dependence of $P(q_\chi)$, together with those of the height of the central peak $P(0)$ and of the side peak $P(q_{\text{EA}})$. These quantities are found to reach stationary values exponentially fast with the correlation time of order of 10^5 MC steps, while actual spin configurations continue to change via the temperature-exchange process and the relatively rapid relaxation realized at higher temperatures.

4. Off-equilibrium simulations

In this section, we report on our results of *off-equilibrium* MC simulations.¹⁶ Unlike the case of equilibrium simulations, the system here is never in full thermal equilibrium. Recent studies have revealed that one can still get useful information from such off-equilibrium simulations, even including certain equilibrium properties. The quantities we are mainly interested here are the off-equilibrium spin and chirality autocorrelation functions defined by

$$C_s(t_w, t + t_w) = \frac{1}{N} \sum_i [\langle \mathbf{S}_i(t_w) \cdot \mathbf{S}_i(t + t_w) \rangle], \quad (4.1)$$

$$C_\chi(t_w, t + t_w) = \frac{1}{3N} \sum_{i,\mu} [\langle \chi_{i\mu}(t_w) \chi_{i\mu}(t + t_w) \rangle]. \quad (4.2)$$

MC simulation is performed based on the standard single spin-flip heat-bath method here. Starting from completely random initial configurations, the system is quenched to a working temperature. Total of about 3×10^5 MC steps per spin are generated in each run. Sample average is taken over 30-120 independent bond realizations, four independent runs being made using different spin initial conditions and different sequences of random numbers for each sample. The lattice size mainly studied is $L = 16$ with periodic boundary conditions, while in some cases lattices with $L = 12$ and 24 are also studied.

The spin and chirality autocorrelation functions at a low temperature $T/J = 0.05$ are shown in Fig. 4 as a function of t . For larger t_w , the curves of the spin autocorrelation function C_s come on top of each other in the long-time regime, indicating that the stationary relaxation is recovered and aging is interrupted. This behavior has been expected because the 3D Heisenberg spin glass has no standard spin-glass order.^{2,3,4,5,6,7,8} By contrast, the chiral autocorrelation function C_χ shows an entirely different behavior: Following the initial decay, it exhibits a clear plateau around $t \sim t_w$ and then drops sharply for $t > t_w$. It also shows an eminent aging effect, namely, as one waits longer, the relaxation becomes slower and the plateau-like behavior at $t \sim t_w$ becomes more pronounced. It should be noticed that the plateau-like behavior observed here has been hardly noticeable in simulations of the 3D EA model.

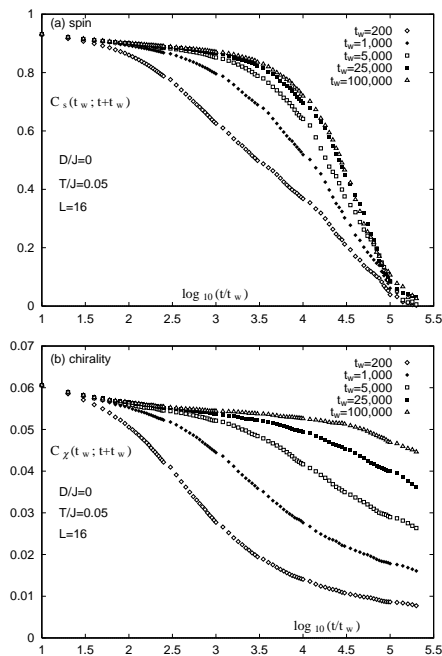


Fig. 4. Off-equilibrium spin (a) and chirality (b) autocorrelation functions at a temperature $T/J = 0.05$ plotted versus $\log_{10} t$ for various waiting times t_w . The lattice size is $L = 16$ averaged over 66 samples.

While the plateau-like behavior observed in C_χ is already suggestive of a nonzero *chiral* Edwards-Anderson order parameter, $q_{CG}^{EA} > 0$, more quantitative analysis similar to the one recently done by Parisi *et al* for the 4D Ising spin glass²¹ is performed to extract q_{CG}^{EA} from the data of C_χ in the quasi-equilibrium regime. Finiteness of q_{CG}^{EA} is also visible in a log-log plot of C_χ versus t as shown in the inset of Fig. 5, where the data show a clear upward curvature. We extract q_{CG}^{EA} by fitting the data of C_χ for $t_w = 3 \times 10^5$ to the power-law form, $C(t_w, t + t_w) = q^{EA} + \frac{C}{t^\alpha}$, in

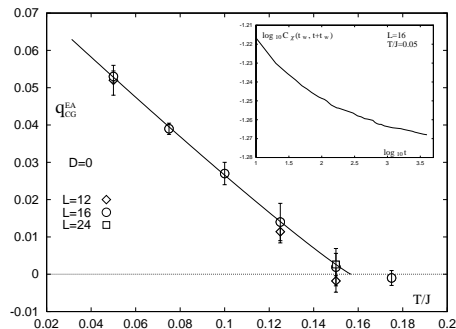


Fig. 5. Temperature dependence of the Edwards-Anderson order parameter of the chirality. The data are averaged over 30-120 samples. Inset exhibits the log-log plot of the t -dependence of the chiral autocorrelation function in the quasi-equilibrium regime for $L = 16$ and $t_w = 3 \times 10^5$.

the time range $40 \leq t \leq 3,000$ satisfying $t/t_w \leq 0.01$. The obtained q_{CG}^{EA} , plotted as a function of temperature in Fig. 5, clearly indicates the occurrence of a finite-temperature chiral-glass transition at $T_{CG}/J = 0.157 \pm 0.01$ with the associated order-parameter exponent $\beta_{CG} = 1.1 \pm 0.1$. The size dependence turns out to be rather small, although the mean values of q_{CG}^{EA} tend to slightly increase around T_{CG} with increasing L . Since both finite-size effect and finite- t_w effect tend to underestimate q_{CG}^{EA} , one may regard the present result as a rather strong evidence of the occurrence of a finite-temperature chiral-glass transition.

The present estimate of the transition temperature $T_{CG}/J = 0.157 \pm 0.01$ is in very good agreement with the equilibrium estimate in the preceding section, $T_{CG}/J = 0.160 \pm 0.005$. If we combine the present estimate of β_{CG} with the estimate of γ_{CG} in the preceding section and use the scaling relations, various chiral-glass exponents can be estimated to be $\alpha \simeq -1.7$, $\beta_{CG} \simeq 1.1$, $\gamma_{CG} \simeq 1.5$, $\nu_{CG} \simeq 1.2$ and $\eta_{CG} \simeq 0.8$. The dynamical exponent is estimated to be $z_{CG} \simeq 4.7$ by using the estimated value of λ and the scaling relation $\lambda = \beta_{CG}/z_{CG}\nu_{CG}$. While the dynamical exponent z_{CG} comes rather close to the z of the 3D Ising EA model, The obtained static exponents differ significantly from those of the 3D Ising EA model $\beta \simeq 0.6$, $\gamma \simeq 4$, $\nu \simeq 2$ and $\eta \simeq -0.35$,^{22,23,24,25,26} suggesting that the universality class of the chiral-glass transition of the 3D Heisenberg spin glass differs from that of the standard 3D Ising spin glass. According to the chirality mechanism, the criticality of real spin-glass transitions is derived from that of the chiral-glass transition of an isotropic Heisenberg spin glass, so long as the magnitude of random anisotropy is not too strong. If one tentatively accepts this scenario, the present result opens up an interesting possibility that the universality class of many of real spin-glass transitions might differ from that of the standard Ising spin glass, contrary to common belief.

5. Conclusion

In summary, spin-glass and chiral-glass orderings of isotropic 3D Heisenberg spin glasses are studied by extensive MC simulations. Clear evidence of the occurrence of a finite-temperature chiral-glass transition without the conventional spin-glass order is presented both by equilibrium and off-equilibrium simulations. Spin and chirality show very different dynamical behaviors consistent with the “spin-chirality separation”. While the spin autocorrelation exhibits only an interrupted aging, the chirality autocorrelation persists to exhibit a pronounced aging effect reminiscent of the one observed in the mean-field model. The universality class of the chiral-glass transition is different from that of the standard Ising spin glass, while the chiral-glass ordered state appears to exhibit a feature of “one-step” replica-symmetry breaking. We expect that these numerical findings have important implications to the understanding of the nature of real spin-glass ordering.

Acknowledgment

We would like to thank Prof. I. Campbell, Prof. A. P. Young and Prof. H. Takayama for useful discussion. The numerical calculation was performed on the Fujitsu VPP500 at the supercomputer center, ISSP, University of Tokyo, on the Hitachi SR2201 at the supercomputer center, University of Tokyo, and on the CP-PACS computer at the Center for Computational Physics, University of Tsukuba.

References

1. For reviews see (a) K. Binder and A. P. Young, *Rev. Mod. Phys.* **58**, 801 (1986); (b) K. H. Fischer and J. A. Hertz, *Spin Glasses* Cambridge University Press (1991); (c) J. A. Mydosh, *Spin Glasses* Taylor & Francis (1993); (d) *Spin glasses and random fields* ed. by A. P. Young, World Scientific, Singapore (1997).
2. J. R. Banavar and M. Cieplak, *Phys. Rev. Lett.* **48**, 832 (1982).
3. W. L. McMillan, *Phys. Rev.* **B 31** 342 (1985).
4. J. A. Olive, A. P. Young and D. Sherrington, *Phys. Rev.* **B34**, 634 (1986).
5. F. Matsubara, T. Iyota and S. Inawashiro, *Phys. Rev. Lett.* **67**, 1458 (1991).
6. H. Kawamura, *Phys. Rev. Lett.* **68**, 3785 (1992).
7. H. Kawamura, *J. Phys. Soc. Jpn.* **64**, 26 (1995).
8. H. Kawamura, *Int. J. Mod. Physics* **7**, 345 (1996).
9. K. Hukushima and H. Kawamura, submitted; H. Kawamura and K. Hukushima, in *Computer Simulation Studies in Condensed Matter Physics XI*, Eds. D. P. Landau and H. B. Schüttler (Springer Verlag, Heidelberg, Berlin, 1998); *J. Magn. Magn. Mater.* **177-181**, 69 (1998).
10. L. Lundgren, P. Svedlinth, P. Nordblad and O. Beckman, *Phys. Rev. Lett.* **51**, 911 (1983).
11. E. Vincent, J. Hammamm, M. Ocio, J-P. Bouchaud and L.F. Cugliandolo, Sitges Conference on Glassy Systems, 1996 (Springer, in press) cond-mat.9607224.
12. J-P. Bouchaud, L. F. Cugliandolo, J. Kurchan and M. Mézard, in *Spin Glasses and Random Fields* (Ref.1(d)).
13. L. F. Cugliandolo and J. Kurchan, *Phys. Rev. Lett.* **71**, 173 (1993).; *J. Phys.* **A27**, 5749 (1994); *Phil. Mag.* **71**, 501 (1995) .
14. J. Villain, *J. Phys.* **C10**, 4793 (1977); **C11**, 745 (1978).
15. K. Hukushima and K. Nemoto, *J. Phys. Soc. Jpn.* **65**, 1604 (1996).

16. H. Kawamura, Phys. Rev. Lett. **80**, 5421 (1998).
17. H. Rieger, J. Phys. A**26**, L615 (1993.); H. Rieger, B. Steckemetz and M. Schreckenberg, Europhys. Lett. **27**, 485 (1994).; J. Kisker, L. Santen, M. Schreckenberg and H. Rieger, Phys. Rev. B**53**, 6418 (1996).
18. A. Baldassarri, Phys. Rev. E **58**, 7047 (1998).
19. H. Takayama, H. Yoshino and K. Hukushima, J. Phys. A**30**, 3891 (1997).
20. E. Marinari, G. Parisi, D. Rossetti, Eur. Phys. J. B (France) **2**, 495 (1998).
21. G. Parisi, F. Ricci-Tersenghi and J. J. Ruiz-Lorenzo, J. Phys. A**29**, 7943 (1996).
22. N. Kawashima and A. P. Young, Phys. Rev. B **53**, R484 (1996).
23. K. Hukushima, H. Takayama and K. Nemoto, Int. J. Mod. Phys. **7**, 337 (1996).
24. E. Marinari, G. Parisi and J. J. Ruiz-Lorenzo, Phys. Rev. B**58**,14852 (1998).; and in *Spin glasses and random fields* (Ref. 1(d)).
25. B. A. Berg and W. Janke, Phys. Rev. Lett. **80**, 4771 (1998).
26. S. Caracciolo and M. Palassini, Phys. Rev. Lett. **82**, 5128 (1999).